A Flexible OLED based VLC Link with *m*-CAP Modulation

Zahra Nazari Chaleshtori[1], Andrew Burton[2], Zabih Ghassemlooy[2], Stanislav Zvanovec[1]

[1]*Deptartment of Electromagnetic Field, Faculty of Electrical Engineering, Czech Technical University in Prague, Prague, Czech Republic, 16627*
[2]*Optical Communications Research Group, Faculty of Engineering and Environment, Northumbria University, Newcastle-upon-Tyne, NE1 8ST, UK*
{nazarzah; xzvanove}@fel.cvut.cz, {z.ghassemlooy; andrew2.burton}@northumbria.ac.uk

***Abstract*—In recent years there has been a growing interest in using organic light emitting diodes (OLEDs) for illumination in indoor environments. They offer attractive features such as flexibility and large active areas at a low cost; they are energy efficient and have higher illumination levels compared to silicone based LEDs. In addition, the utilization of OLEDs have increased in devices such as smart mobile phones and TVs because of their low thickness. This paper investigates the performance of an OLED based visible light communications (OVLC) system, using a curved and flat OLED with multiband carrierless amplitude and phase (*m*-CAP) modulation for *m* = 2 at different angles of incidence on the optical receiver. It is shown that the BER performance is improved (i.e., below the forward error correction (FEC) limit of 3.8×10^{-3}) with the curved OLED when the optical receiver moving along a circular path for the viewing angles greater 40^{o} compared to the flat OLED, which is advantageous in device to device communications.**

Keywords- flexible organic LEDs; m-CAP modulation; visible light communications.

I. INTRODUCTION

Visible light communications (VLC) simultaneously provides illumination and wireless data transmission using the visible spectrum of 380 nm to 750 nm [1, 2]. VLC is a green technology and can offer advantages over the radio frequency (RF) communication systems such as immunity to RF electromagnetic interference, a license-free spectrum, inherent security, and lower power consumption [1, 3]. VLC systems employ either conventional silicone based light emitting diodes (LEDs), organic based LEDs (OLEDs) or even white laser diodes (LDs) as light sources [4]. The applications of VLC has been increasing due to the widespread use of LEDs as the light sources in indoor and outdoor environments. For example, indoor positioning systems [5], aviation [6], underwater communications [6], intelligent transportation systems [7], internet of things (IoT) [8] and camera communications [9].

There has been a growing interest into adopting OLEDs over the conventional solid-state lights. Flat panel OLED displays are attractive due to properties such as the possibility of fabricating the device on flexible substrates, achieving larger active areas using low-cost solution processing techniques and environmentally friendly (i.e., a green technology) [4]. Organic electronics are able to use plastics as the substrates, hence can be made to be mechanically flexible and with arbitrary shapes. This allows for the production of curved or rolled OLED panels/displays, which can also be employed in wearable products (i.e., smart watches and wearable computers). In addition, the maximum thickness of an OLED is 500 nm [4], which is ideal for thin film devices (such as mobile phones, computers, and TVs), thus providing the potential of infrastructure-to-device (I2D) and device-to-device (D2D) communications [9]. In D2D communications, the data can be transmitted via pixels of the mobile phones display [10] and is captured using the camera(s) in smartphones [11].

However, the reported modulation bandwidth B_{mod} of OLEDs is lower than silicone LEDs (i.e., kHz compared to MHz), which is limited by the carrier lifetime [12]. Recent improvements of the OLEDs properties are showing that with new materials increased charge mobility can be achieved [13]. The performance of organic devices is dependent on the charge mobility, i.e., as charge carrier mobility determines how fast the device can be turned on and off. Recently, a number of advanced communication techniques and signalling schemes have been proposed to increase the transmission data rates R_b. A significant enhancement in R_b from 550 kb/s [14] to more than 50 Mb/s was reported for OLED-based visible light communication (OVLC) [15]. An almost 55 Mb/s OLED link was reported in [16] where wavelength-division multiplexing (WDM) (using red/orange, blue and green wavelengths) and an artificial neural network (ANN) equalizer was used. In [17], a 51.6 Mb/s experimental monochromic OLED based VLC system was demonstrated; where the OLED modulated by offset-quadrature amplitude modulation-based orthogonal frequency division multiplexing (OFDM) was employed with a joint linear minimum mean-square-error (LMMSE) based decision feedback equalizer (DFE). Furthermore, employing polymer LEDs (PLEDs) in the VLC systems has shown a notable enhancement in R_b, as reported in [18]. For instance, 10 Mb/s was achieved using PLED (having B_{mod} of 270 kHz) and on-off keying (OOK) in combination with a least mean square (LMS) equalizer [19], reaching the same R_b as OFDM organic VLC system [20]. Next, through low-temperature thermal annealing and crystallisation of the polymer, a marginal improvement in B_{mod} up to 350 kHz has been reported in [18] with R_b of 20 Mb/s using an ANN equalizer. In [21], a fully organic flexible VLC system using off-the-shelf components, flexible circuits and flexible commercial OLED and an organic photodiode (PD) - manufactured in a roll-to-roll process - was reported. This all-organic flexible VLC

system is capable of transmitting an audio file in real-time. And their future goal is to design the driving circuits operating over hundreds of MHz, both in emission and transmission, and to build an OPD that could support this operating frequency.

The use of advanced modulation schemes to improve the spectral efficiency of bandlimited VLC systems are being investigated [20]. OFDM has the potential for supporting high order modulation formats such as quadrature amplitude modulation (QAM), where both amplitude and phase components were used to achieve spectrum efficiency [22]. Multiband carrierless amplitude and phase (*m*-CAP) also employs QAM, and is based on a combination of two pulse amplitude modulation (PAM) signals to form a QAM signal and their impulse responses form a Hilbert pair. CAP modulation has been the focus of increasing research in recent years due to a number of advantages including high spectral efficiency. In this paper a flexible OLED is proposed as a light source for *m*-CAP VLC, which can be used in short range device to device communications in a number of indoor applications. We characterize the OLED to determine the illumination profile and power current relationship. The link performance is quantified in terms of the bit error rate (BER).

The rest of the paper is organized as follows. In Section II, the structure of OLEDs is described. Section III discusses the experimental set-up. Section IV experimental results. Finally, conclusions are given in Section IV.

II. The Structure of OLEDs

The structure of an OLED consists of a substrate (glass, metal or plastic) to which all other layers are deposited, metal cathodes and anode, the organic photoactive layers and an external light extraction film, see Fig. 1 [1]. The organic layers are sandwiched between a transparent anode (indium tin oxide (ITO)) and a metal cathode (aluminium or silver) [1]. The organic materials can be long-chain polymers (i.e., PLEDs) or small organic molecules (i.e., SMOLEDs) in a crystalline phase [12]. Using flexible substrates, such as polyethylene terephthalate, provides OLED panels or displays that can be curved or rolled. These are used in wearable products, mobile phones, and TVs. As the production cost drops, non-rigid OLED lighting products begin to offer a competitive advantage over LED and other lighting technologies.

OLEDs have a low-pass filter transfer function with the cut-off frequency given by [1]:

$$f_c = \frac{1}{2\pi RC}, \tag{1}$$

where R is the effective resistance of the OLED and C is the plate capacitance expressed by [1]:

$$C = \frac{A\varepsilon_0\varepsilon_r}{d}, \tag{2}$$

where A is the OLED photoactive area, d is the OLED thickness, and ε_0 and ε_r are the permittivity of free space and relative dielectric constant of the organic layer, respectively.

According to (1) and (2), f_c is inversely proportional to the photoactive area; consequently, a larger photoactive area decreases the achievable B_{mod} and a restriction in R_b is imposed on OVLC systems. Moreover, in bandlimited systems, inter-symbol interference (ISI) leads to BER degradation. In addition, high pass filtering or capacitive coupling leads to deviating the signal randomly from the DC level called the baseline wander (BLW), which is another challenge in OVLC systems. A number of techniques have been proposed to improve OVLC systems performance. For instance, high-level modulation schemes [20] and equalization using ANN [18].

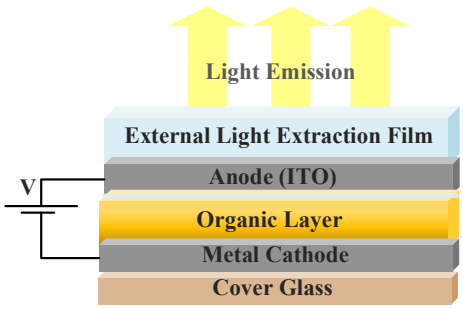

Fig. 1. An OLED structure

III. Experimental Set-Up

A block diagram of a *m*-CAP OVLC link is shown in Fig. 2. First, m independent pseudo-random data streams $d_m(t)$ (where $m = 2$) with the length of 12,000 bits are generated and mapped onto the QAM constellation. Note, in this work 16-QAM is considered. The real $\Re(a_i)$ and imaginary $\Im(b_i)$ components of the upsampled data are applied to their corresponding filters. Here we use square root raised cosine (SRRC) filters with carrier frequencies of 10 kHz (s_1 the first subcarrier) and 30 kHz (s_2 the second subcarrier) with the corresponding in-phase and quadrature components modulated onto the sine and cosine waves, respectively. The roll-off factor used for for the root-raised the sine and cosine pulses is 0.15, as to stay with the literature. The filters outputs are summed, which represent the *m*-CAP signal $x(t)$ and is used for intensity modulation of the OLED via the output driver. At the receiver, following optical detection and amplification the regenerated electrical signal $y(t)$ is applied to the bit and frame synchronization module, and the output of the module is applied to two filters of g_I and g_Q which are the time-reversed SRRC filters used at the transmitter. The summed filters output signal $z(t)$ is downsampled and is fed to the M-QAM demapper to obtain the estimates transmitted data $d'_m(t)$.

The experimental test-bed for the proposed link uses a flexible OLED, which is depicted in Fig. 3. The *m*-CAP signal was supplied using an Agilent arbitrary function generator (AFG 3252). The *m*-CAP signal was generated in the Matlab domain. The required sampling frequency and a number of samples per symbol can be determined following the procedures outlined in [23] and the references within. The optical receiver (ORx) consists of a PD and a transimpedance amplifier (TIA) (Thorlabs PDA100A2). The flexible OLED panel has been bent with a curvature radius r of 11 cm, see Fig 4. Here we considered two cases for system evaluation: (i) the ORx moving along a fixed radius of h = 30 cm around the light source, (case1) see Fig. 4(a);

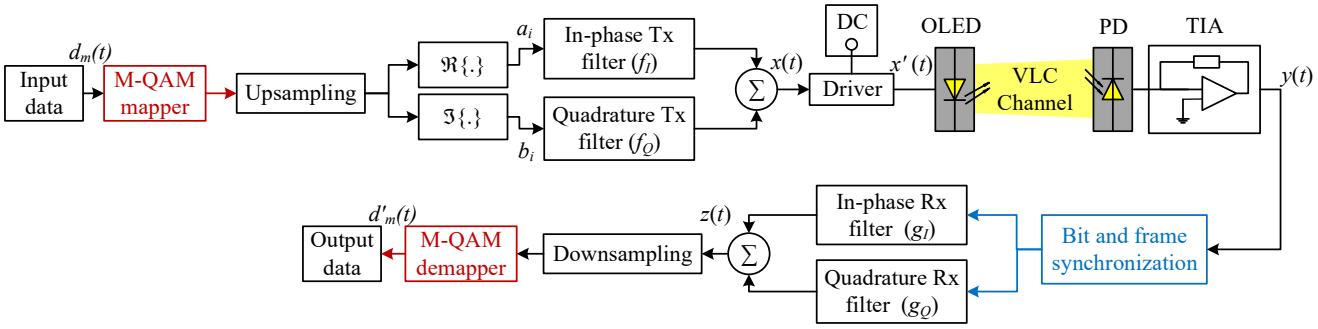

Fig. 2. The block diagram of the proposed system with *m*-CAP modulation.

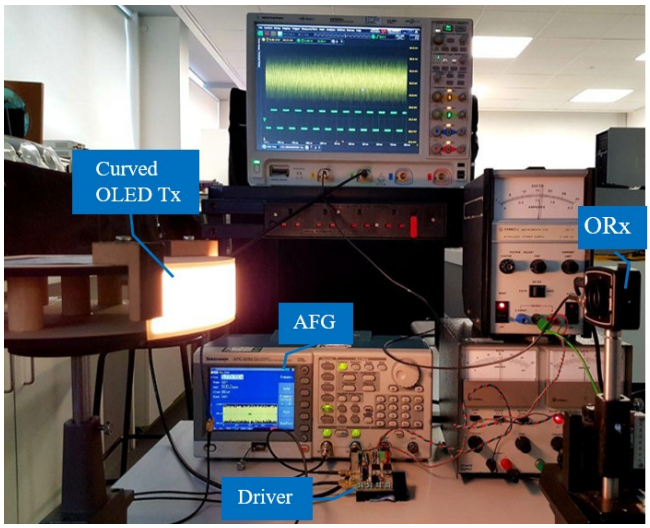

Fig. 3. An OVLC experimental test-bed with a curved OLED

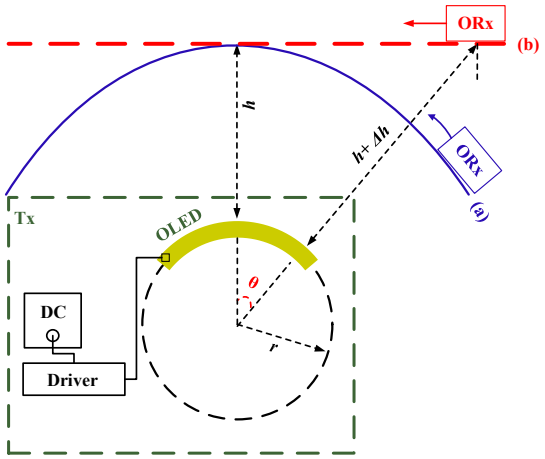

Fig. 4. The block diagram of the experimental set-up with the ORx moving along; (a) a circular path (case1) and (b) a staight path (case2).

and (*ii*) the Rx was placed on the axis in parallel to the light source, (case2) see Fig. 4(b). We measured the BER for both curved and flat OLEDs over the two scenarios. All the key system parameters are shown in Table I.

TABLE I. THE SYSTEM PARAMETERS

Equipment	Parameter	Value
OLED	Dimension	200 ×50 mm^2
	Type	flexible
	Bandwidth	43 (kHz)
	Maximum current	300 (mA)
	Bias current	160 (mA)
	Voltage amplitude	600 (mV)
	Threshold voltage	7 (V)
	Flux	75 (lm)
	Luminous efficacy	50 to 55 (lm/W)
Channel	Length	30 cm
ORx	Active area	75.4 mm^2
	Bandwidth	1.4 MHz at a 10 dB gain
	Output voltage	0 to 10 V
	Noise of amplifier	195 μV (RMS)
	NEP	6.75×10^{-12} (W/$\sqrt{\text{Hz}}$) at λ= 960 nm

IV. Experimental Results

A. *Characterization of flexible OLED*

The measured normalized optical spectrum (normalized to the maximum achieved intensity associated with the highest I_B) of the OLED at different bias currents I_B is depicted in Fig. 5(a), which shows the individual red, green and blue (RGB) components at the peak wavelengths of 620 nm (R), 555 nm (G), 450 nm and 480 nm (B). Next, we normalised the intensity plots shown in Fig. 5(a) to unity and then superimposed on top of each other with the result shown in Fig. 5(b). The plot reveals that the OLED has the same spectral distribution over a wide range of I_B

(i.e., 10-300 mA), thus, the emitted spectrum is independent of I_B and the dimming levels.

The measured *L-I-V* curve of OLED is shown in Fig. 6, and the optical power displays a highly linear response over a wide current dynamic range of 22 dB (between 10-300 mA). Using linear curve-fitting the power $P_I = 2.4\ I_B + 20$, which gives optical power (mW) associated with each I_B (mA), is defined. To measure the output optical power of OLED, an optical power meter (PM100D Thorlabs, S120VC 200-1100 nm 50 mW) with a narrow band optical blue filter with a transmissivity of > 0.96, which was positioned at a distance 15 times greater than the OLED length in order to ensure a point source light at the far field was used. To determine the optical power P_I at specific values of I_B, we used $P_I = \alpha P_m$, where P_m is the measured power and α can be given by $\alpha = P_t/P_o$. P_t and P_o are the total area under the spectrum profile associated to I_B and area under the blue component, respectively. In Fig. 6, the inset shows a uniform illumination profile for the OLED along its length.

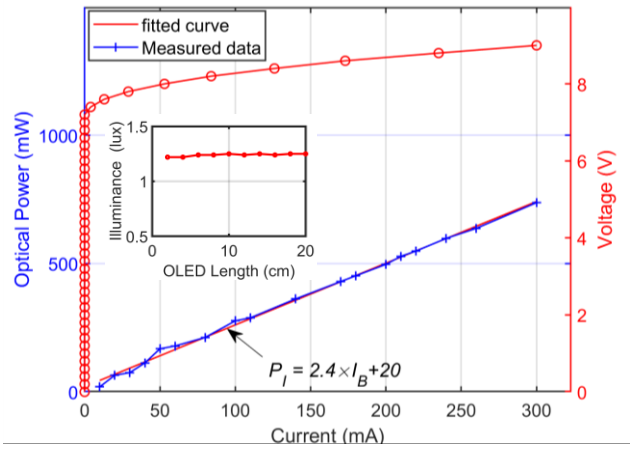

Fig. 6. The *L-I-V* curves for flexible OLED. The illumination profile along the OLED length is shown in inset.

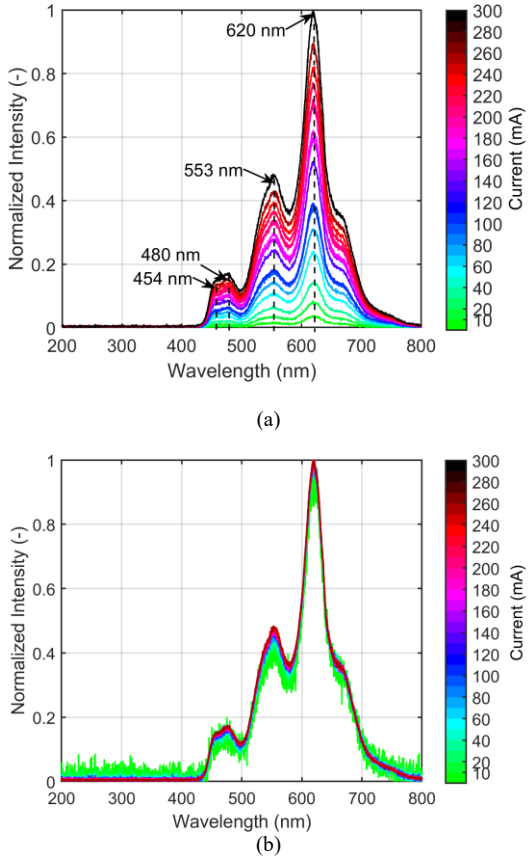

Fig. 5. (a) The optical spectrum of the flexible OLED under test with peak wavelengths marked where the legend color scale represents I_B, and (b) the spectrum of the OLED at different I_B corresponding to different dimming levels. Each of the spectral responses were normalized to unity and then superimposed on top of each other.

B. M-CAP modulation for OVLC link with flexible OLED

Fig. 7 demonstrates the polar plots of the BER for the proposed *m*-CAP OVLC system for s_1 and s_2 for both the flexible and flat OLEDs and for the circular path (see Fig. 4(a)). Also shown for reference is the forward error correction (FEC) BER limit of 3.8×10^{-3}. As illustrated, the BER display a symmetry about the origin (i.e., The ORx is facing the OLED at θ of 0°) due to uniform illumination profile of OLED referred to the inset plot in Fig. 6 (i.e., the same signal to noise ratio (SNR) across the entire face of OLED). As can be seen, the BER for the curved OLED is improved over a wider θ compared to the flat OLED because of fixed transmission range between the ORx and the OLED. Note, for the circular path the BER remains just below the FEC limit for θ within the range of ±78° and ±50° for the curved and flat OLEDs, respectively and for s_1. However, for s_2, θ drops by 17° and 8° for the curved and flat OLED, respectively.

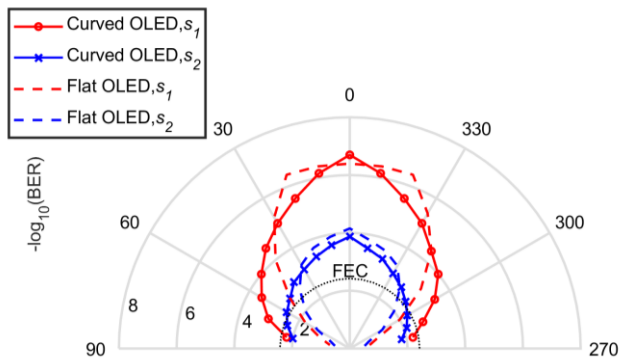

Fig. 7. The polar curve of BER for *m*-CAP with s_1 and s_2 for case1 (i.e., when the circular paths of ORx with respect to the OLED) for curved and flat OLED.

The BER versus the angle θ for the straight path for s_1 and s_2 are shown in Fig. 8. In this case, θ are 30° and 42° to meet the FEC limit for the curved and flat OLEDs, respectively for s_1. Note that, for the straight path the transmission distance between the ORx and the transmitter increase by Δh when moving away from the centre point (i.e., $\theta = 0$). To consider this, Fig. 9 depicts the BER versus Δh for curved and flat OLED (note, $\Delta h = 0$ corresponds to the centre point of OLED). As shown, for the flat OLED and for s_1, the BER remains below the FEC limit for -7 cm < Δh < 10 cm, while for the curved OLED the distance of ORx is in the range of -5 cm < Δh < 5 cm. The results show that, the potential of using the flexible OLEDs in D2D communications, display-based communications, etc., where the viewing position is not problematic.

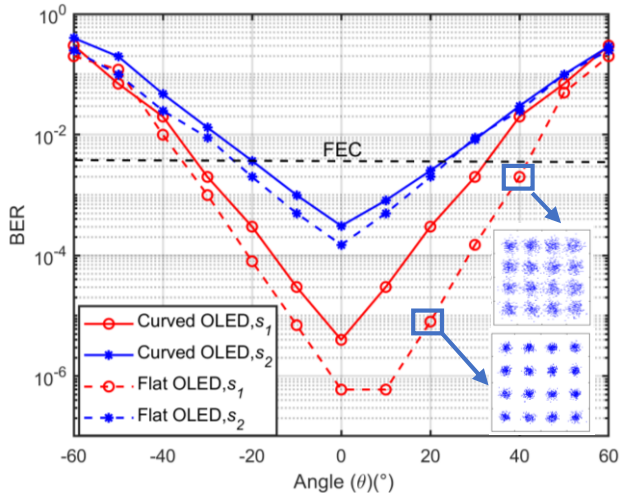

Fig. 8. The BER versus the angle θ for the case2 for curved and flat OLED with m-CAP and for s_1 and s_2. Note, the straight paths of ORx with respect to the OLED are referred to as case2.

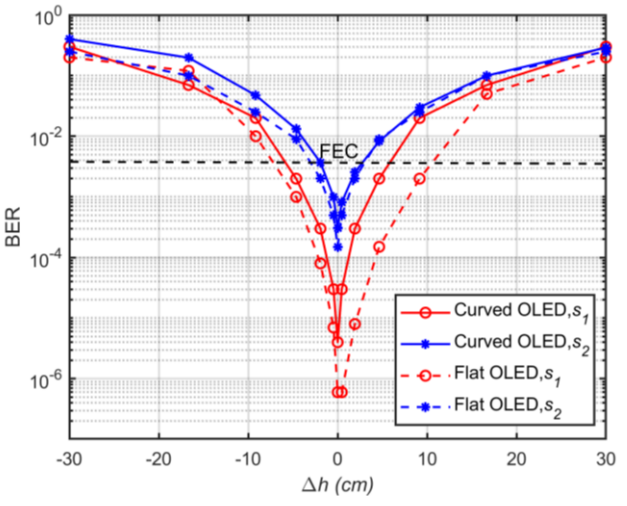

Fig. 9. The BER versus the Δh for m-CAP with s_1 and s_2; for curved and flat OLED for the case2. Note, the straight path of ORx with respect to the OLED is referred to as case2.

V. Conclusion and Future Outlook

In this paper, we proposed m-CAP VLC using a flexible OLED as the transmitter. We carried out the characterization of the OLED and showed that, it has a highly linear power-current relationship and there were no changes in the colour as a function of the current over a wide range (i.e., 10-300 mA). The link BER performance was measured and compared with a flat OLED based m-CAP VLC. It was shown that the curved OLED with the optical receiver moving along a circular path offered improved BER performance (i.e., below the FEC limit) over a wide viewing angle for a single subcarrier based m-CAP VLC. This work demonstrated the potential of utilizing flexible OLED based VLC in short range device to device communications.

Acknowledgement

The work is supported by the European Union's Horizon 2020 research and innovation programme under the Marie Sklodowska-Curie grant agreement no 764461 (VISION) and the Czech Rep. funded project GACR 17-17538S and the UK EPSRC grant EP/P006280/1: MARVEL.

Reference

[1] Z. Ghassemlooy, L. N. Alves, S. Zvanovec, and M.-A. Khalighi, *Visible Light Communications: Theory and Applications*. CRC Press, 2017.

[2] Z. Ghassemlooy, W. Popoola, and S. Rajbhandari, *Optical wireless communications: system and channel modelling with Matlab®*. 2nd Edition. CRC press, NY, 2019.

[3] B. Lin, X. Tang, Z. Ghassemlooy, C. Lin, and Y. Li, "Experimental demonstration of an indoor VLC positioning system based on OFDMA," *IEEE Photonics Journal,* vol. 9, no. 2, pp. 1-9, 2017.

[4] P. A. Haigh, Z. Ghassemlooy, S. Rajbhandari, and I. Papakonstantinou, "Visible light communications using organic light emitting diodes," *IEEE Communications Magazine,* vol. 51, no. 8, pp. 148-154, 2013.

[5] H. Lv, L. Feng, A. Yang, P. Guo, H. Huang, and S. Chen, "High accuracy VLC indoor positioning system with differential detection," *IEEE Photonics Journal,* vol. 9, no. 3, pp. 1-13, 2017.

[6] D.-R. Kim, S.-H. Yang, H.-S. Kim, Y.-H. Son, and S.-K. Han, "Outdoor visible light communication for inter-vehicle communication using controller area network," in *2012 Fourth International Conference on Communications and Electronics (ICCE)*, 2012: IEEE, pp. 31-34.

[7] T. Nguyen, A. Islam, and Y. M. Jang, "Region-of-interest signaling vehicular system using optical camera communications," *IEEE Photonics Journal,* vol. 9, no. 1, pp. 1-20, 2017.

[8] S. Schmid, T. Richner, S. Mangold, and T. R. Gross, "EnLighting: An indoor visible light communication system based on networked light bulbs," in *2016 13th Annual IEEE International Conference on Sensing, Communication, and Networking (SECON)*, 2016: IEEE, pp. 1-9.

[9] Y. Li, Z. Ghassemlooy, X. Tang, B. Lin, and Y. Zhang, "A VLC smartphone camera based indoor positioning system," *IEEE Photonics Technology Letters,* vol. 30, no. 13, pp. 1171-1174, 2018.

[10] R. Boubezari, H. Le Minh, Z. Ghassemlooy, and A. Bouridane, "Smartphone camera based visible light communication," *Journal of Lightwave Technology,* vol. 34, no. 17, pp. 4121-4127, 2016.

[11] B. Lin, Z. Ghassemlooy, C. Lin, X. Tang, Y. Li, and S. Zhang, "An indoor visible light positioning system based on optical camera communications," *IEEE Photonics Technology Letters,* vol. 29, no. 7, pp. 579-582, 2017.

[12] C.-H. Hsiao, C.-F. Lin, and J.-H. Lee, "Driving voltage reduction in white organic light-emitting devices from selectively doping in ambipolar blue-emitting layer," *Journal of Applied Physics,* vol. 102, no. 9, p. 094508, 2007.

[13] W. Zhu *et al.*, "Graphene radio frequency devices on flexible substrate," *Applied Physics Letters,* vol. 102, no. 23, p. 233102, 2013.

[14] P. A. Haigh *et al.*, "Exploiting equalization techniques for improving data rates in organic optoelectronic devices for visible light communications," *Journal of lightwave technology,* vol. 30, no. 19, pp. 3081-3088, 2012.

[15] Z. N. Chaleshtori, P. Chvojka, S. Zvanovec, Z. Ghassemlooy, and P. A. Haigh, "A Survey on Recent Advances in Organic Visible Light Communications," in *2018 11th International Symposium on Communication Systems, Networks & Digital Signal Processing (CSNDSP)*, 2018: IEEE, pp. 1-6.

[16] P. A. Haigh *et al.*, "Wavelength-multiplexed polymer LEDs: Towards 55 Mb/s organic visible light communications," *IEEE Journal on Selected Areas in Communications,* vol. 33, no. 9, pp. 1819-1828, 2015.

[17] H. Chen, Z. Xu, Q. Gao, and S. Li, "A 51.6 Mb/s Experimental VLC System Using a Monochromic Organic LED," *IEEE Photonics Journal,* vol. 10, no. 2, pp. 1-12, 2018.

[18] P. A. Haigh *et al.*, "A 20-Mb/s VLC link with a polymer LED and a multilayer perceptron equalizer," *IEEE Photonics Technology Letters,* vol. 26, no. 19, pp. 1975-1978, 2014.

[19] P. A. Haigh *et al.*, "Visible light communications: real time 10 Mb/s link with a low bandwidth polymer light-emitting diode," *Optics express,* vol. 22, no. 3, pp. 2830-2838, 2014.

[20] S. T. Le *et al.*, "10 Mb/s visible light transmission system using a polymer light-emitting diode with orthogonal frequency division multiplexing," *Optics letters,* vol. 39, no. 13, pp. 3876-3879, 2014.

[21] C. Vega-Colado *et al.*, "An All-Organic Flexible Visible Light Communication System," *Sensors,* vol. 18, no. 9, p. 3045, 2018.

[22] M. S. Islim *et al.*, "Towards 10 Gb/s orthogonal frequency division multiplexing-based visible light communication using a GaN violet micro-LED," *Photonics Research,* vol. 5, no. 2, pp. A35-A43, 2017.

[23] M. I. Olmedo *et al.*, "Multiband carrierless amplitude phase modulation for high capacity optical data links," *Journal of Lightwave Technology,* vol. 32, no. 4, pp. 798-804, 2014.